

Analytical equation for the motion picture response time of display devices

Fenglin Peng,^{1,a)} Haiwei Chen,^{1,a)} Fangwang Gou,¹ Yun-Han Lee,¹ Michael Wand,² Ming-Chun Li,³ Seok-Lyul Lee,³ and Shin-Tson Wu^{1,b)}

¹College of Optics and Photonics, University of Central Florida, Orlando, Florida 32816, USA

²LC Vision, 4150 Darley Ave., Suite 10, Boulder, Colorado 80305, USA

³AU Optronics Corporation, Hsinchu Science Park, Hsinchu 300, Taiwan

(Received 4 December 2016; accepted 31 December 2016; published online 12 January 2017)

Motion picture response time (MPRT) affects the image blurs of thin-film transistor (TFT) liquid crystal displays and organic light emitting diode (OLED) displays. We derive an analytical equation to correlate MPRT with the liquid crystal (LC)/OLED response time and TFT frame rate. Good agreement between our physical model and experimental results is obtained. Based on our model, we find that if the LC's response time is 2 ms or less, then its MPRT is nearly the same as that of OLED, even if OLED's response time is assumed to be 0. To achieve MPRT comparable to OLEDs, we developed an ultra-low viscosity LC mixture for the vertical alignment mode operation. The measured average gray-to-gray response time is 0.93 ms, and its MPRT at 120 Hz is 6.88 ms. In comparison, OLED's MPRT is 6.67 ms. To further shorten MPRT, we could either increase the frame rate or reduce the backlight duty ratio. Pros and cons of these approaches are discussed. *Published by AIP Publishing.* [<http://dx.doi.org/10.1063/1.4974006>]

I. INTRODUCTION

After more than three decades of extensive material research, device development, and heavy investment on advanced manufacturing technologies, thin-film-transistor liquid crystal displays (TFT LCDs) have become ubiquitous in our daily lives.¹ Its widespread applications span from TVs, monitors, tablets, to smartphones. In addition, displays for gaming monitors and virtual reality (VR) systems are growing rapidly, which demand a higher resolution density, more vivid colors, and unnoticeable image blur. Lately, "LCD versus OLED (organic light emitting diode), who wins?" is a heated debate topic.^{2,3} Each technology has its own merits and demerits. Generally speaking, LCD is leading in lifetime, peak brightness, and cost; it is comparable to OLED in resolution density, power consumption, ambient contrast ratio, and viewing angle but inferior to OLED in black state, panel flexibility, color gamut, and response time. Therefore, LCD camp has devoted a great deal of efforts to narrow the performance gap against OLED, including quantum-dot backlight^{4,5} for achieving wider color gamut and lower power consumption, and local dimming⁶ to enhance the dynamic contrast ratio to 1 000 000:1. The remaining grand challenge for LCDs is the response time; especially, nematic LCDs suffer $\sim 100\times$ slower response time than OLED (~ 0.1 ms). Thus, it is commonly perceived that LCDs exhibit more severe image blurs than OLEDs for the fast-moving objects.³ To improve the LC response time, several approaches have been investigated, e.g., polymer-stabilized blue phase LCs,^{7,8} low viscosity nematic LCs,^{9–11} and ferroelectric LCs.¹² Nevertheless, it remains challenging for nematic LCs to achieve ~ 0.1 ms while keeping a low operation voltage.

The image blur of a TFT LCD (or OLED) is governed by two important parameters: the LC (or OLED) response time and TFT sample and the hold time. Motion Picture Response Time (MPRT)^{13,14} has been proposed to quantify the visual performance of a moving object as

$$\text{MPRT (ms)} = \text{BEW (pixel)} / v (\text{pixel/frame}) \times T_f (\text{ms/frame}). \quad (1)$$

Here, BEW stands for the perceived blurred edge width, which is proportional to the object's moving speed (v), and T_f is the TFT's frame time (unit: ms), which is the inverse of frame rate (f , unit: Hz)

$$f = 1000 / T_f. \quad (2)$$

Both TFT LCDs and OLEDs are hold-type displays, which means the displayed image is hold on by TFTs in a given frame time. As a result, they both suffer from different degree of image blurs, depending on the frame rate and the response time. That is, to say, OLED could still exhibit motion blurs even if its response time is zero.¹⁵ Recently, Chen *et al.*¹⁶ reported a fast-LCD with MPRT comparable to OLED, but the physical origin of MPRT is not discussed. Unlike LCD and OLED, CRT (the cathode ray tube) is an impulse-type display, whose MRPT ≈ 1.5 ms and is free from motion blur.¹⁷ The required MPRT depends on the specific applications. For example, if a smartphone or monitor is mainly intended for static images, then a slow MPRT does not affect the display performance. But to clearly display an object moving at speed $v = 480$ pixels per second, the required MPRT should be less than 4 ms. If the speed doubles, then the required MPRT should be faster than 2 ms. Presently, most LCD and OLED TVs are operated at 120 Hz (i.e., MPRT ~ 6.66 ms); thus, image blur remains noticeable for the fast-moving objects. There is an urgent

^{a)}F. Peng and H. Chen contributed equally to this work.

^{b)}Electronic mail: swu@ucf.edu

need to reduce MPRT to ~ 1.5 ms (or faster) to eliminate motion blurs. To obtain such a fast MPRT, several approaches have been proposed¹⁴ such as: (1) employing a pursuit camera to reproduce the BEW and then calculate the MPRT based on Eq. (1) and (2) using the time based image integration to simulate it. However, these methods are less straightforward and even require complicated experimental setups.

In this paper, we analyze the origin of MPRT and derive a simple equation to correlate the MPRT with the LC response time and the TFT frame rate. Therefore, the MPRT can be calculated easily based on the measured LC response time and the operation frame rate. Good agreement is obtained between the equation, rigorous simulation results, and experimental results. Through our analyses, we find that if the LC's response time is 2 ms or less, then its MPRT is nearly the same as that of OLED, even if OLED's response time is assumed to be 0. In the experiment, we prepared three ultra-low viscosity LC mixtures and used them in the vertical alignment (VA) mode¹⁸ for TVs and the fringing field switching (FFS) mode¹⁹ for smartphones. With the overdrive and undershoot driving scheme, the measured average gray-to-gray (GTG) response time is only 0.93 ms for the VA cell and 2.95 ms for the FFS cell, and their average GTG MPRT is comparable to that of OLED at the same frame rate. By increasing the frame rate and/or decreasing the backlight duty ratio, we can achieve MPRT < 1.5 ms.

II. SIMULATION MODEL

Figure 1(a) illustrates a simple example about the eye tracking a bright moving object on a dark background. Here, the display is a hold-type display,²⁰ i.e., the object is still on the panel within one frame time and jumps to another position with the speed v . However, human eyes smoothly pursuit the object with the speed v_h . Generally, we assume that $v_h = v$. This discrepancy between the hold-type display and human vision system results in image blurs on retina. The perceived motion picture blur (Fig. 1(b)) is determined by the sum of the pixel's intensity along the motion trajectory within one frame period. The position-dependent luminance curve is plotted in Fig. 1(b), and the blurred edge width is defined as the space interval between 10% and 90% luminance change.²¹ The BEW depends on the moving speed: the faster the moving speed, the more severe image blurs a human eye can observe. To determine MPRT, several approaches have been investigated, such as employing the pursuit camera method and using time based image integration.¹⁴ The pursuit camera approach can reproduce the BEW and calculate the MPRT by using Eq. (1); however, how the LC response affects the MPRT cannot be extracted quantitatively through this method. On the other hand, the time based image integration approach has been demonstrated to be a better way to correlate the liquid crystal response curve (LCRC) with the motion picture response curve (MPRC).

MPRC is related to the LC response curve in conjunction with eye-tracking and temporal integration as follows:^{22,23}

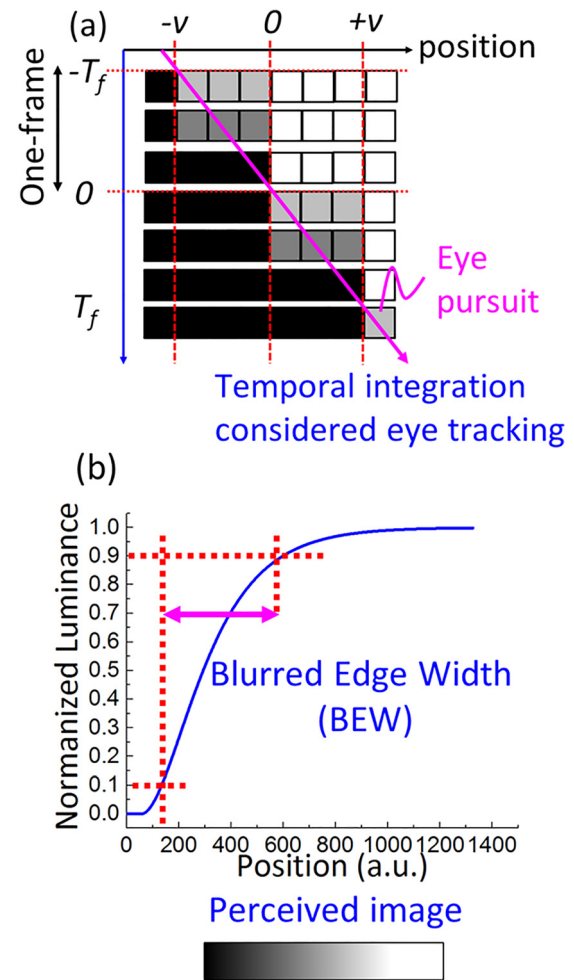


FIG. 1. (a) Illustration of the eye tracking a moving bright object on a dark background. (b) The perceived image blur and position dependent normalized luminance.

$$MPRC(t) = \frac{1}{T_f} \int_t^{t+T_f} T(t') dt'. \quad (3)$$

In Eq. (3), MPRC represents the normalized luminance profile of the blurred image in the temporal domain and $T(t')$ is the output time-dependent transmittance curve, which is jointly determined by the LC response curve and backlight modulation. Figures 2(a) and 2(b) depict the output time-dependent transmittance curve without and with backlight modulation, respectively. MPRC(t) can be derived from the output time-dependent transmittance by applying the one-frame-time moving window function (Fig. 2(c)) as²³

$$MPRC(t) = \frac{1}{T_f} \times [T(t) * H(T_f)], \quad (4)$$

where $*$ denotes the convolution operation and $H(T_f)$ is the rectangle function with width of T_f .

Let us first consider the simplest case without backlight modulation. Under such condition, $T(t)$ is simply the LC response curve. For a VA cell, the time-dependent optical decay curve $T_{LC_decay}(t)$ has been solved analytically as²⁴

$$T_{LC_decay}(t) = \sin^2 \left(\frac{\delta_0 \exp(-2t/\tau_0)}{2} \right), \quad (5)$$

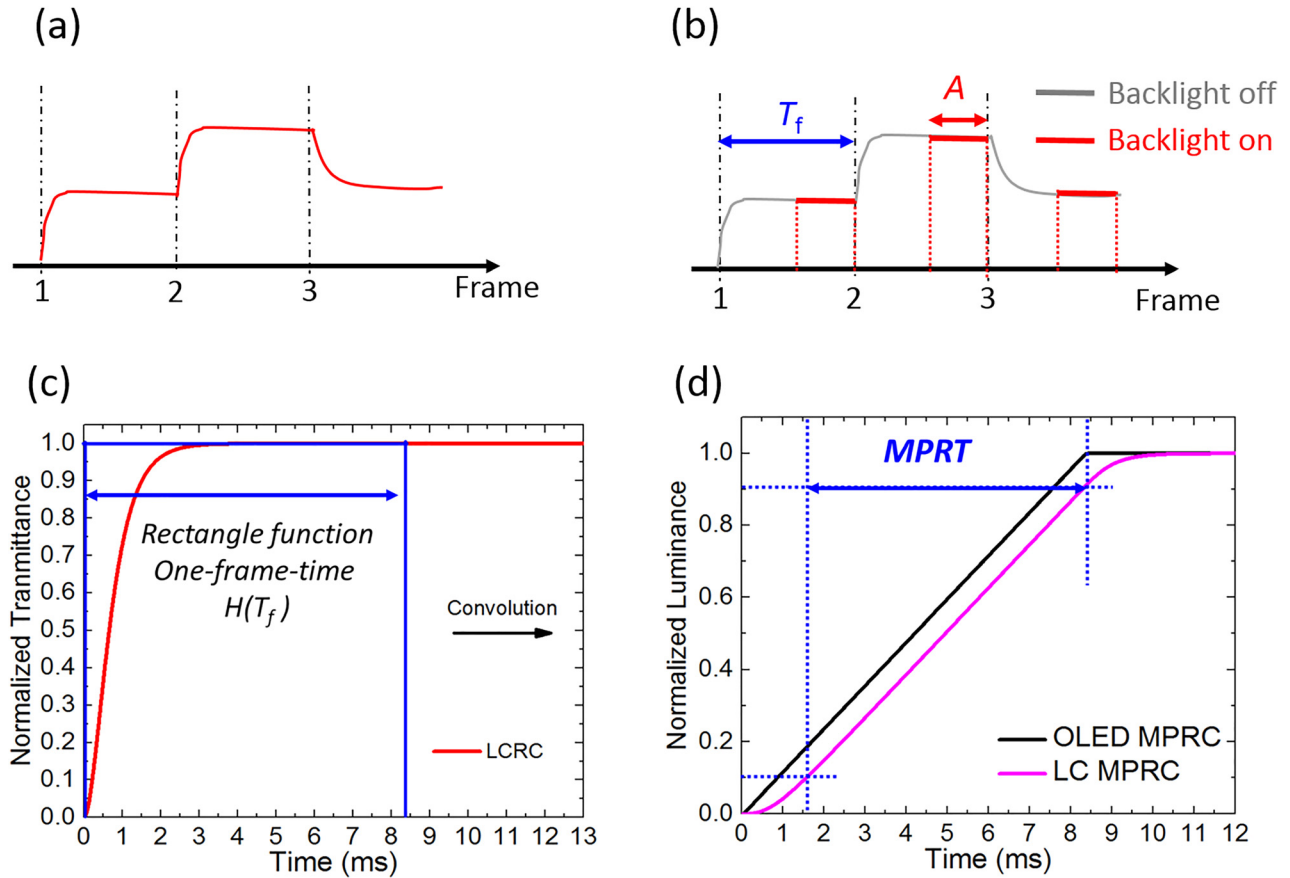


FIG. 2. Illustration of the output time-dependent transmittance curve on hold-type displays: (a) without backlight modulation and (b) with backlight modulation. The duty ratio of backlight is A/T_f . (c) LC response curve and one-frame-time moving window. (d) Illustration of MPRC of LC and OLED at $f=120$ Hz and the starting point $t_0=0$.

$$\tau_0 = \frac{\gamma_1 d^2}{K_{33} \pi^2}, \quad (6)$$

where δ_0 is the phase retardation change, τ_0 stands for the LC director reorientation time, which is determined by the LC visco-elastic coefficient (γ_1/K_{33}) and cell gap d . However, τ_0 is difficult to measure directly. In the experiment, we measure the LC optical response time (τ), which is defined as the time interval between 10% and 90% transmittance change. For a VA cell under small angle approximation, the optical decay time $\tau_d = a\tau_0$, where $a \approx 0.3-0.4$, depending on the initial δ_0 value.²⁴

On the other hand, the optical rise curve ($T_{LC_rise}(t)$) of the VA cell is much more complicated because it also depends on the applied voltage²⁴

$$T_{LC_rise}(t) = \sin^2 \left(\frac{\delta_0/2}{1 + \left[\frac{\phi_\infty^2}{\phi_0^2} - 1 \right] \exp\left(-\frac{2t}{\tau_r}\right)} \right), \quad (7)$$

$$\tau_r = \frac{\tau_0}{\left| \left(\frac{V}{V_{th}} \right)^2 - 1 \right|}. \quad (8)$$

In Eqs. (7) and (8), ϕ_∞ and ϕ_0 represent the tilt angle at $t \rightarrow \infty$ and $t=0$, V is the applied voltage, and V_{th} is the threshold voltage. From Eq. (8), the rise time could be slow when V is

slightly above V_{th} . To overcome this shortcoming, the overdrive and undershoot voltage method²⁵ has been commonly used to speed up the rise time. Therefore, the LC response time is mainly limited by the decay time. Eq. (3) can be derived from the LC response curve by applying the one-frame-time moving window function. Therefore, the starting point of MPRC is affected by the tailing transmittance of the previous frame, which makes the MPRC calculation more complicated. To elucidate the derivation procedures without losing its generality, let us assume that the rise-response curve is symmetric to the decay curve (i.e., $\tau_r = \tau_d$)

$$T_{LC_rise}(t) = \begin{cases} 0; & \text{for } t < t_0 \\ 1 - \sin^2 \left(\frac{\delta_0 \exp(-2(t-t_0)/\tau_0)}{2} \right); & \text{for } t \geq t_0. \end{cases} \quad (9)$$

That means at $t=t_0$, the LCD is switched from the darkest state ($T=0$) to the brightest state ($T=1$), and the transition time is equal to that of decay process. Therefore, the MPRC can be obtained by simultaneously solving Eqs. (9) and (4). In Fig. 2(d), the MPRC of OLED is also included as the benchmark for comparison, and we assume its response time is 0. Similar to the LC response time, MPRT is also defined as the time interval between 10% and 90% luminance change, as Fig. 2(d) depicts.

Substituting Eq. (9) into Eq. (4), we find

$$MPRC(t) = \begin{cases} \frac{1}{T_f} \int_{t_0}^{t_0+t} T_{LC-rise}(t') dt'; & \text{if } t_0 \leq t \leq T_f + t_0, \\ \frac{1}{T_f} \int_t^{t+T_f} T_{LC-rise}(t') dt'; & \text{if } t > T_f + t_0. \end{cases} \quad (10)$$

To simplify the derivation process, let us assume $t_0 = 0$. After Taylor's expansion and only keeping the first and second order terms, we derive the following time-dependent MPRC:

$$MPRC(t) \approx \begin{cases} \frac{1}{T_f} \left\{ t + \frac{\pi^2 \tau_0}{16} \left[\exp\left(-\frac{4t}{\tau_0}\right) - 1 \right] \right\}; & \text{for } 0 < t \leq T_f, \\ \frac{1}{T_f} \left\{ T_f + \left(\frac{\pi^2 \tau_0}{16}\right) \exp\left(-\frac{4t}{\tau_0}\right) \left[1 - \exp\left(\frac{4T_f}{\tau_0}\right) \right] \right\}; & \text{for } t \geq T_f. \end{cases} \quad (11)$$

MPRT can be obtained by taking the time interval between 10% and 90% luminance change. From Eq. (11), we find that MPRT is jointly determined by the LC response time ($\tau \approx \alpha\tau_0$) and the TFT frame time (T_f). In general, we can use the numerical method to plot the MPRC [Eq. (11)] and then obtain the MPRT. But it would be highly desirable if we can derive an analytical expression for MPRT and comprehend how the LC response time and TFT frame time affect MPRT.

To obtain an analytical solution, let us first consider two extreme conditions without backlight modulation: $\tau \rightarrow 0$ and $\tau \gg T_f$. When the LC response time is very fast, we set $\tau_0 \rightarrow 0$, and Eq. (11) is simplified as

$$MPRC(t) = \begin{cases} t/T_f, & \text{if } t < T_f \\ 1, & \text{if } t \geq T_f. \end{cases} \quad (12)$$

Such a MPRC is plotted in Fig. 2(d) (black line). From Fig. 2(d), we find the limiting MPRT $\approx 0.8T_f$. Note: the coefficient 0.8 originates from the MPRT definition, which is from 10% to 90% luminance change. Under such a condition, as the TFT frame rate (f) increases (i.e., T_f decreases), the limiting MPRT decreases linearly. On the other hand, if the TFT frame rate is so fast that the LC cannot follow, i.e., $\tau \gg T_f$, the one-frame time window can be regarded as a pulse function, and Eq. (4) can be simplified as

$$MPRC(t) \approx T(t) * \delta(t) = T(t). \quad (13)$$

Therefore, MPRC overlaps with the LC response curve ($T(t)$), i.e., MPRT $\approx \tau$, which is independent of the frame rate and is solely determined by the LC response time.

To satisfy these two boundary conditions, based on the eye pursuit tracking diagram shown in Fig. 1(a), we propose the following equation to correlate MPRT with the LC response time (τ) and the frame time (T_f):

$$MPRT \approx \sqrt{\tau^2 + (0.8T_f)^2}. \quad (14)$$

To validate Eq. (14), we compare the MPRT results with the simulated ones without approximation. Results are plotted in Fig. 3(a), where the solid lines represent Eq. (14) at the specified frame rates, and the dots are the simulation results using Eqs. (4) and (9) without approximation. The agreement between the rigorous simulation and Eq. (14) is very good. With Eq. (14), we can see easily how the LC response time and the TFT frame rate affect MPRT.

From Fig. 3(a), we find three important trends: (1) At a given frame rate, say, 120 Hz, as the LC response time decreases, MPRT decreases almost linearly and then gradually saturates. Note that the MPRT for $\tau = 2$ ms is only 4% longer than that of $\tau = 0$. Therefore, if an LCD's response time is 2 ms, then its MPRT is comparable to that of an OLED, even if the OLED's response time is assumed to be 0. (2) As the TFT frame rate increases, the limiting MPRT (assuming $\tau = 0$) decreases linearly, because the limiting MPRT $= 0.8T_f$. (3) If the LC response time is not fast enough, say, $\tau = 5$ ms, then increasing the frame rate from 60 Hz to 120 Hz makes a big improvement in MPRT, but further increasing the frame rate to 240 Hz and 480 Hz, the improvement is less obvious. This prediction is consistent with those observed experimentally.²⁶

Besides the LC response time, the other factor affecting the output transmittance $T(t)$ is the backlight modulation, as depicted in Figs. 2(a) and 2(b), where A stands for the time that backlight (e.g., LED) is turned on in the one frame time. The duty ratio (DR) is defined as

$$DR = A/T_f. \quad (15)$$

The MPRC can be calculated numerically using Eq. (4). As $T(t)$ becomes discontinuous in one frame and it is determined jointly by the LC response time and the backlight modulation, so that it is quite complicated to get the analytical expression for MPRC. If the LC response time is fast (e.g., $\tau \leq 2$ ms), then the LC directors can achieve a final gray-level when the backlight is turned on. Thus, $T(t)$ can be

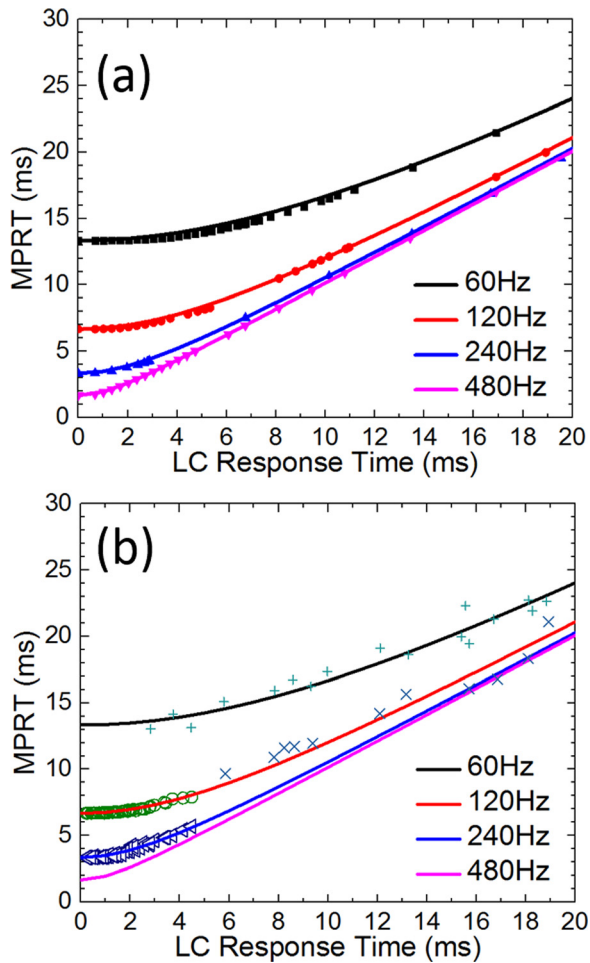


FIG. 3. (a) The LC response time vs. MPRT. Solid lines represent the calculated results from Eq. (14) and dots are simulation results using Eqs. (4) and (9). (b) Open circles and triangles are experimental data measured with the HCCH VA mode at $f=120$ Hz and 240 Hz. Pluses and crosses are experimental data reported in Ref. 14.

simplified by the periodic rectangle function [red lines in Fig. 2(b)]. After taking the convolution, MPRC increases with time linearly. Therefore, the MPRT can be expressed as

$$MPRT \approx 0.8 \times T_f \times DR = 800 \times DR/f. \quad (16)$$

From Eq. (16), we can achieve a fast MPRT by reducing the duty ratio or increasing the frame rate. We will discuss the effects of the duty ratio later.

III. EXPERIMENTAL RESULTS

To validate our findings, we measured the MPRT of two commonly employed LC modes: VA and FFS. Multi-domain VA LCDs have been widely used in large-size TVs and monitors because of their high contrast ratio and low operation voltage. On the other hand, the FFS mode has advantages in a wide view, weak color shift, and pressure resistance for touch panels. Thus, the FFS mode is commonly used in touch panel displays, such as smartphones and tablets. Depending on the sign of dielectric anisotropy ($\Delta\epsilon$), FFS can be categorized into positive type (p-FFS) and negative type (n-FFS).²⁷

TABLE I. Chemical structures of the components in MX-40702.

#	Chemical structures
1	
2	
3	
4	
5	
6	

A. Material development

Table I lists the compound structures employed in the LC mixture, designated as MX-40702. Six major ingredients are included. The homologues ($R=1-5$) of compound 1, compounds 2 and 3 show large dielectric anisotropy and high clearing point. Their clearing points range from 160 °C to 190 °C, which help to widen the nematic range. However, their viscoelastic coefficient and activation energy are relatively large, as the molecules are quite long and bulky. Therefore, components 4 and 5 are doped to reduce the viscosity. Component 5 also introduces a strong lateral dipole with the 2,3-difluoroaryl group, which helps to maintain a reasonable $|\Delta\epsilon|$. In addition, we added component 6 ($R=0$ to 3 carbon alkyl chain) to lower the threshold voltage and melting point.

We also prepared another negative LCs, HCCH 736700-100 (abbreviated as HCCH; provided by HCCH, China). The clearing point is higher than 100 °C, so it can be employed for the applications at extreme environments, such as vehicle and outdoor displays. These two negative $\Delta\epsilon$ LCs can be used in VA and n-FFS modes. In the experiment, we filled MX-40702 and HCCH into two VA cells ($d=3.3 \mu\text{m}$) and two n-FFS cells ($d=3.3 \mu\text{m}$). Besides, a positive $\Delta\epsilon$ LC (DIC-LC2)²⁸ was also used for investigating the MPRT of p-

TABLE II. Physical properties of the four LC mixtures at $T=22$ °C and $\lambda=550$ nm.

LCs	T_m (°C)	T_c (°C)	Δn	$\Delta\epsilon$	K_{11} (pN)	K_{22} (pN)	K_{33} (pN)	γ_1 (mPaS)
MX-40702	<-40	70	0.105	-2.4	...	5.5	13.7	69.4
HCCH	<-40	102	0.121	-2.2	...	5.3	19.8	93.0
DIC-LC2	<-40	75	0.121	2.0	12.5	6.5	13.5	31.7

FFS cell ($d=3.6\ \mu\text{m}$). The physical properties of these three mixtures are summarized in Table II, including the melting point (T_m), clearing point (T_c), dielectric anisotropy ($\Delta\epsilon$), birefringence (Δn), elastic constants (K_{11} , K_{22} , and K_{33}), and rotational viscosity (γ_1).

B. LC response time and MPRT

In Fig. 3(b), we plot the GTG LC response time vs. MPRT at $f=120\ \text{Hz}$ (open circles) and $240\ \text{Hz}$ (triangles) for the HCCH VA cell. The overdrive and undershoot method was applied to achieve faster response time. For the convenience of discussion, let us assume the switching takes place between gray level 2 and gray level 5. During the rising period, we applied a maximum available voltage for a short period ($\sim 1\ \text{ms}$) to accelerate the LC directors from level 2 to level 5, and then followed by a holding voltage to keep the transmittance at gray level 5. To achieve the fast decay time, we removed the voltage of gray level 5 for a short period and then followed by a holding voltage to keep the transmittance at gray level 2. By doing so, we can shorten the rise time and

decay time by $2\times-3\times$. The solid lines in Fig. 3(b) represent Eq. (14) at four different frame rates. A good agreement is obtained between the experiment and Eq. (14). We also include the experimental data taken at $f=60\ \text{Hz}$ and $120\ \text{Hz}$ from Ref. 14 for comparison. A good agreement is also found.

Figures 4(a)–4(d) show the measured GTG LC response time and its corresponding MPRT at $f=120\ \text{Hz}$ for VA cells with MX-40702 and HCCH. For n-FFS and p-FFS modes, the measured GTG LC response time and MPRT are plotted in Figs. 5(a)–5(d). Table III summarizes the average GTG LC response time and MPRT at different frequencies. In our VA cell with MX-40702 (and HCCH), its average GTG response time is $0.93\ \text{ms}$ (and $1.56\ \text{ms}$), which is $6.1\times$ (and $3.6\times$) faster than that of a commercial LCD.³ The average GTG MPRT of both VA cells is only $\sim 3\%$ slower than that of OLED at the same frame rate (e.g., $f=120\ \text{Hz}$). That is, to say, these VA LCDs exhibit a comparable motion image blurs to OLEDs, except for some slower gray level transitions, e.g., from gray level 8 to 1. Besides, HCCH has a slightly higher birefringence; thus, its required cell gap can be reduced to $d\sim 3\ \mu\text{m}$. By doing so, the response time can

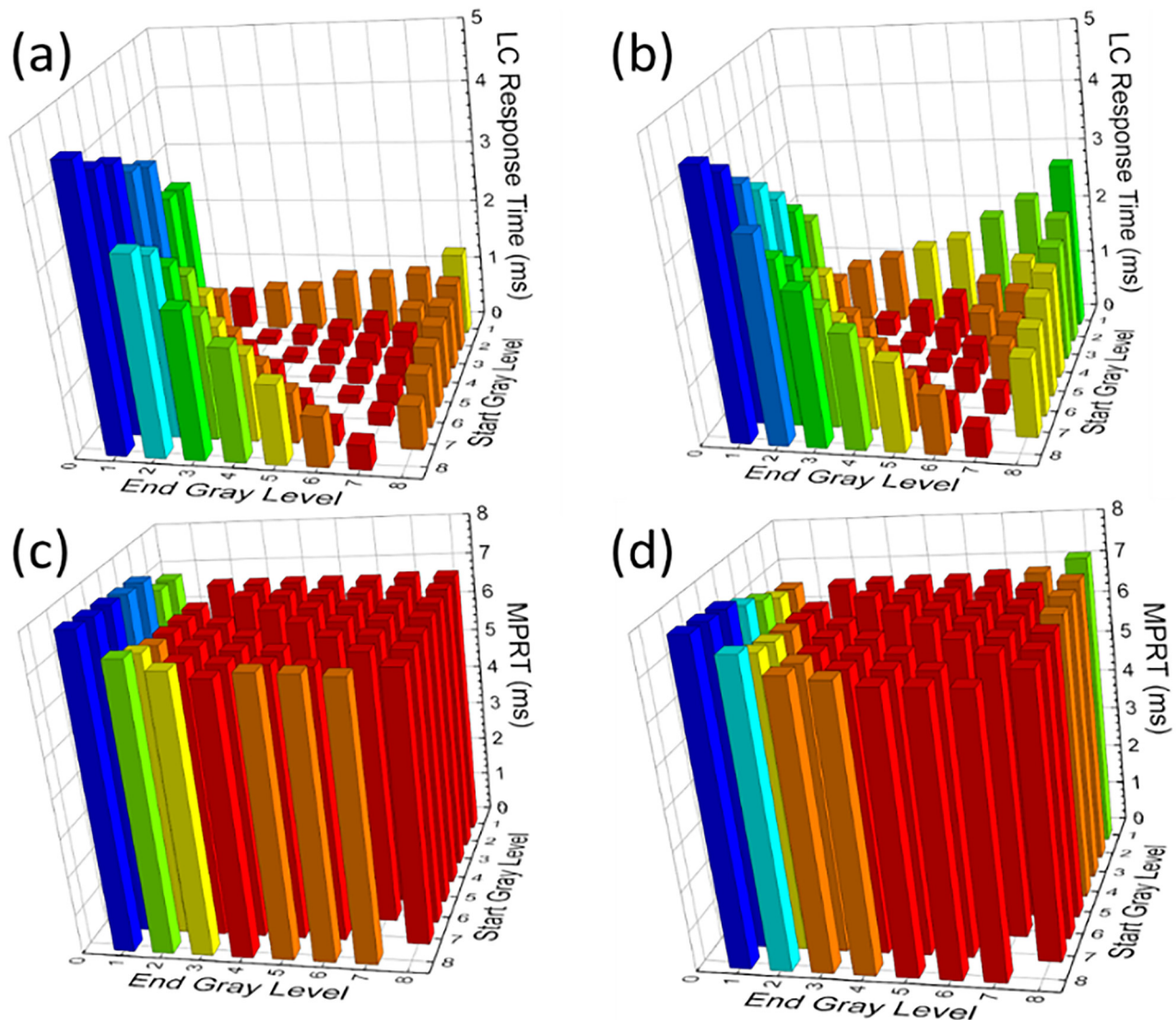


FIG. 4. For VA mode, the measured GTG LC response time of (a) MX-40702 and (b) HCCH. The corresponding GTG MPRT at $f=120\ \text{Hz}$ for (c) MX-40702 and (d) HCCH.

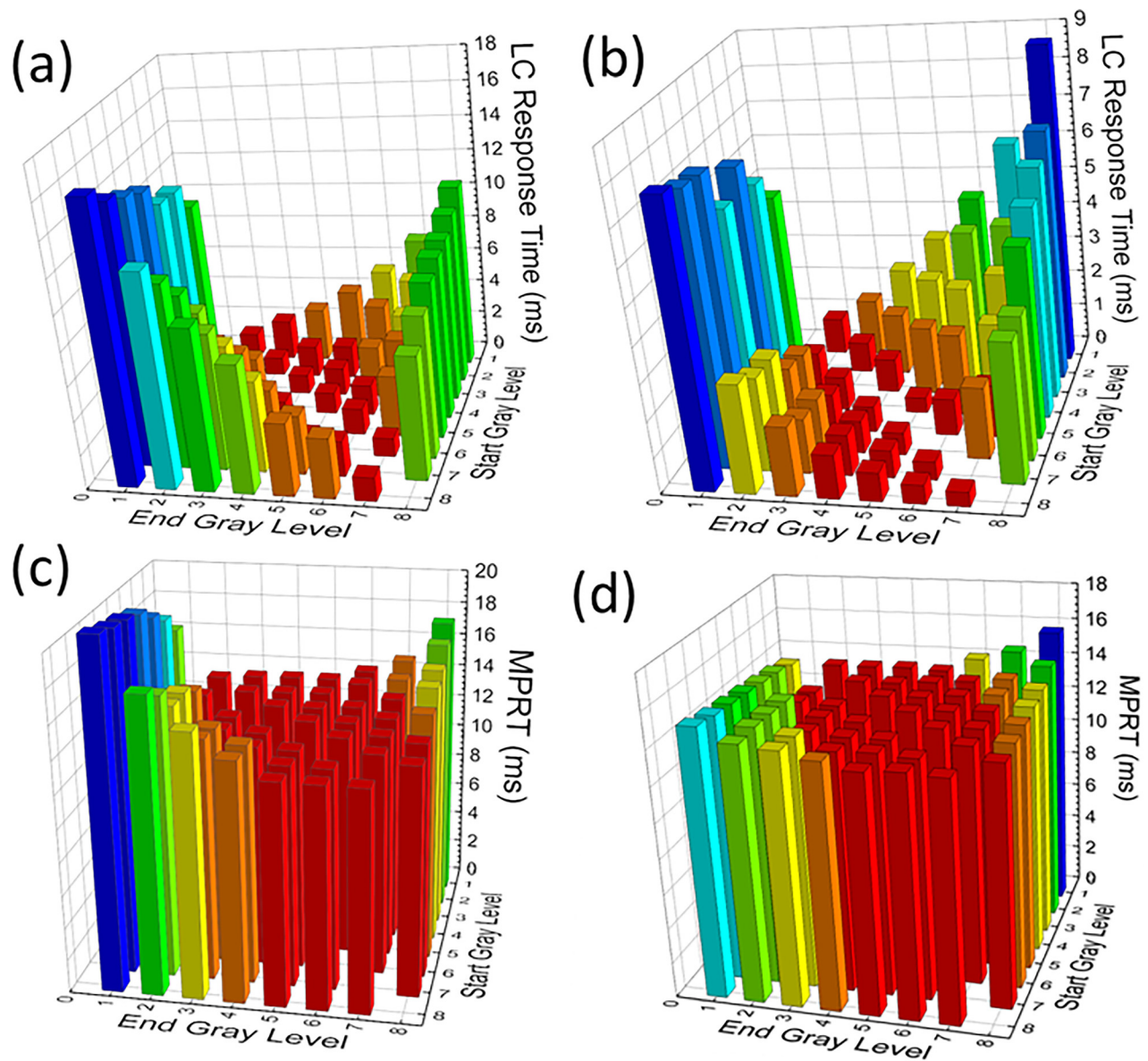


FIG. 5. The GTG LC response time with (a) MX-40702 for n-FFS and (b) DIC-LC2 for p-FFS. The GTG MPRT at $f=60$ Hz for (c) MX-40702 and (d) DIC-LC2.

be reduced by $\sim 20\%$. For mobile phones and tablets, using the FFS mode, the frame rate is $f=60$ Hz or lower in order to reduce the power consumption. From Table III, at $f=60$ Hz, the MPRT of p-FFS and n-FFS is 3% and 12% slower than that of OLED, respectively. However, the mobile phones and tablets are intended for static images, which do not need fast MPRT. Therefore, LCD and OLED

exhibit comparable image performance in terms of motion picture blurs for TV and monitors.

IV. DISCUSSION

To further reduce image blurs, here we present three approaches: higher frame rate, backlight modulation, and a

TABLE III. On-state voltage, average GTG LC response time and MPRT for different LCDs and OLED.

LCs	On-state voltage V_{on} (V)	Average GTG LC response time (ms)	Average GTG MPRT $f=60$ Hz (ms)	Average GTG MPRT $f=120$ Hz (ms)	Average GTG MPRT $f=240$ Hz (ms)	
VA	MX-40702	7.5	0.93	13.40	6.80	3.58
VA	HCCH	7.6	1.56	13.46	6.87	3.77
p-FFS	DIC-LC2	7.5	2.95	13.83	7.49	4.74
n-FFS	MX-40702	7.0	5.90	15.03	9.40	7.10
OLED	...		0.10	13.33	6.67	3.33

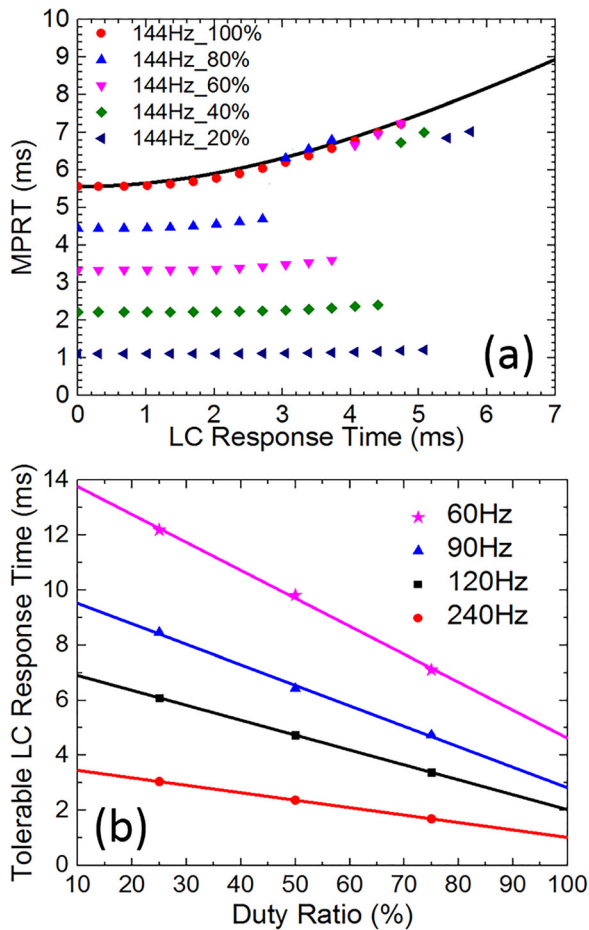


FIG. 6. (a) LC response time vs. MPRT with different duty ratios at $f=144$ Hz. (b) Duty ratio vs. tolerable LC response (τ_T) at different frame rates.

combination of both. From Table III, if the frame rate is increased from 120 Hz to 240 Hz, the MPRT of VA LCD and OLED is reduced by $\sim 2\times$ yet remaining comparable (3.58 ms vs. 3.33 ms). A major tradeoff of higher frame rate is the increased electronic power consumption.

The second approach to reduce MPRT is through backlight modulation. Figure 6(a) shows the simulation results of LC response time dependent MPRT with different duty ratios. The frame rate is $f=144$ Hz, which is presently the highest frame rate employed in commercial products, such as gaming monitors. The limiting MPRT (i.e., $\tau=0$) is reduced linearly when the backlight duty ratio decreases, as Eq. (16) shows. The reasons are twofold: (1) The slow transition part of LC is obscured by the delayed backlight, and (2) the sample-and-hold effect is suppressed because such an operation mechanism is similar to CRT's impulse driving. As a matter of fact, to suppress image blurs Sony's OLED TVs also employed 50% duty ratio,¹⁵ because MPRT decreases linearly with the duty ratio. To minimize an LCD's motion blur for high-speed gaming or sports, the targeted MPRT is 1.5 ms, similar to CRT. As Fig. 6(a) shows, if we raise the frame rate to 144 Hz and reduce the duty ratio to 20%, then the MPRT is ~ 1.1 ms. A low duty ratio helps to shorten MPRT, but the major tradeoff is the decreased brightness and the decreased power efficiency. To compensate for the brightness loss, we can boost the current of the LED backlight. For OLED, in

principle, we can do the same impulse driving. However, high current impulse driving of OLED leads to substantial efficiency roll-off²⁹ and lifetime degradation.³⁰ Similarly for LCD, high current driving of blue LED also suffers from the droop effect,³¹ i.e., the internal quantum efficiency declines as the current density increases. Fortunately, the impact of droop effect on LED is substantially weaker than the declined efficiency and compromised lifetime to OLED. That is to say, OLED is much more vulnerable than LCD to impulse driving. As a matter of fact, the impulse driving of LCD has been attempted using black image insertion or blinking backlight more than a decade ago.³²⁻³⁴ The improvement was indeed substantial, except that the intrinsic LC response time was slow (~ 20 ms) so that the blurs were still noticeable.

The third approach to achieve much faster MPRT is to combine the high frame rate with backlight modulation. From Eq. (16), if we increase the frame rate to 240 Hz while keeping duty ratio at $\sim 45\%$, then we can achieve $MPRT \approx 1.5$ ms. However, the electronic power consumption is increased linearly with the frame rate. On the other hand, boosting the LED current to compensate for the brightness loss due to backlight modulation could also result in a slightly higher power consumption because of the droop effect. For a 55-in. LCD TV, the electronic part consumes $\sim 10\%$ of total power, while the backlight shares the rest 90%. Therefore, to improve the power efficiency with fast MPRT, the higher frame rate with the larger duty ratio is preferred for large-size LCD applications. But for a 5-in. smartphone, the electronic and optical parts contribute nearly equally. Therefore, a proper combination between the frame rate and duty ratio should be optimized, depending on the specific applications.

As depicted in Fig. 6(a), at a certain frame rate and duty ratio, there exists an abrupt jump of MPRT as the LC response time increases. The LC response time at the jump is defined as the tolerable LC response time (τ_T). Therefore, to achieve a comparable MPRT to that of OLED with the same duty ratio, the LC response time should be $\tau \leq \tau_T$. For example, at $f=144$ Hz, to achieve ~ 1 ms MPRT, the required duty ratio is 20% and $\tau_T \sim 5.1$ ms. Since the average GTG response time of both VA (with MX-40702 or HCCH) and p-FFS (DIC-LC2) are all less than 5 ms, MPRT ~ 1 ms can be achieved by a proper combination between the frame rate and duty ratio.

Figure 6(b) shows the tolerable LC response time at each duty ratio for different frame rates. As depicted, τ_T increases linearly as the duty ratio decreases. This is because the longer LC transition process is not perceived when the backlight is off. For displays without backlight modulation, τ_T can be obtained by extrapolating the line shown in Fig. 6(b), which helps us to determine the acceptable LC response time for different frame rates. When $\tau \leq \tau_T$, the MPRT increases with the LC response time slowly ($<6\%$), which is a rather negligible change compared to the limiting MPRT. Therefore, it shows comparable image performance to OLED in terms of motion picture blur. On the other hand, for $\tau > \tau_T$, the MPRT increases with the LC response time linearly. The corresponding MPRT can be calculated using Eq. (14) easily.

V. CONCLUSION

In summary, we reported two negative $\Delta\varepsilon$ LCs with a small visco-elastic coefficient. For VA LCDs, the average MPRT is comparable to that of OLED at the same frame rate. Faster MPRT can be obtained by increasing the frame rate, reducing the backlight duty ratio, and the combination of both. Using $f = 144$ Hz and 20% duty ratio or $f = 240$ Hz and $\sim 45\%$ duty ratio, we can achieve MPRT < 1.5 ms to display fast-moving objects without motion blurs. On the other hand, for mobile displays, FFS modes with our LC mixtures also exhibit a similar MPRT to that of OLED at $f \leq 60$ Hz.

ACKNOWLEDGMENTS

The authors are indebted to Air Force Office for Scientific Research (under Grant No. FA9550-14-1-0279) and A.U. Vista, Inc., for financial supports, DIC Corporation, Japan, for providing DIC-LC2 mixture, and Professor Jiun-Haw Lee, Dr. Zhenyue Luo, Dr. Daming Xu, and Mr. GuanJun Tan for helpful discussions.

¹M. Schadt, *Jpn. J. Appl. Phys.* **48**, 03B001 (2009).

²Y. Ukai, *SID Symp. Dig. Tech. Pap.* **44**, 28 (2013).

³J. K. Yoon, E. M. Park, J. S. Son, H. W. Shin, H. E. Kim, M. Yee, H. G. Kim, C. H. Oh, and B. C. Ahn, *SID Symp. Dig. Tech. Pap.* **44**, 326 (2013).

⁴Y. Shirasaki, G. J. Supran, M. G. Bawendi, and V. Bulović, *Nat. Photonics* **7**, 13 (2013).

⁵Z. Luo, D. Xu, and S.-T. Wu, *J. Display Technol.* **10**, 526 (2014).

⁶H. Chen, T. H. Ha, J. H. Sung, H. R. Kim, and B. H. Han, *J. Soc. Inf. Disp.* **18**, 57 (2010).

⁷H. Kikuchi, M. Yokota, Y. Hisakado, H. Yang, and T. Kajiyama, *Nat. Mater.* **1**, 64 (2002).

⁸F. Peng, Y. Chen, J. Yuan, H. Chen, S.-T. Wu, and Y. Haseba, *J. Mater. Chem. C* **2**, 3597 (2014).

⁹H. Chen, M. Hu, F. Peng, J. Li, Z. An, and S.-T. Wu, *Opt. Mater. Express* **5**, 655 (2015).

¹⁰F. Peng, Y. Huang, F. Gou, M. Hu, J. Li, Z. An, and S.-T. Wu, *Opt. Mater. Express* **6**, 717 (2016).

¹¹F. Peng, F. Gou, H. Chen, Y. Huang, and S. T. Wu, *J. Soc. Inf. Disp.* **24**, 241 (2016).

¹²A. K. Srivastava, V. G. Chigrinov, and H. S. Kwok, *J. Soc. Inf. Disp.* **23**, 253 (2015).

¹³T. Kurita, *SID Symp. Dig. Tech. Pap.* **32**, 986 (2001).

¹⁴Y. Igarashi, T. Yamamoto, Y. Tanaka, J. Someya, Y. Nakakura, M. Yamakawa, S. Hasegawa, Y. Nishida, and T. Kurita, *SID Symp. Dig. Tech. Pap.* **34**, 1039 (2003).

¹⁵H. Ito, M. Ogawa, and S. Sunaga, *J. Vision* **13**, 6 (2013).

¹⁶H. Chen, F. Peng, F. Gou, Y.-H. Lee, M. Wand, and S.-T. Wu, *Optica* **3**, 1033 (2016).

¹⁷A. Sluyterman, *J. Soc. Inf. Disp.* **14**, 681 (2006).

¹⁸M. Schiekel and K. Fahrenschon, *Appl. Phys. Lett.* **19**, 391 (1971).

¹⁹S. H. Lee, S. L. Lee, and H. Y. Kim, *Appl. Phys. Lett.* **73**, 2881 (1998).

²⁰D. Sasaki, M. Imai, and H. Hayama, *SID Symp. Dig. Tech. Pap.* **33**, 926 (2002).

²¹Y. Igarashi, T. Yamamoto, Y. Tanaka, J. Someya, Y. Nakakura, M. Yamakawa, Y. Nishida, and T. Kurita, *SID Symp. Dig. Tech. Pap.* **35**, 1262 (2004).

²²W. Song, X. Li, Y. Zhang, Y. Qi, and X. Yang, *J. Soc. Inf. Disp.* **16**, 587 (2008).

²³W. Song, K. Teunissen, X. Li, Y. Zhang, and I. Heynderickx, *J. Soc. Inf. Disp.* **17**, 251 (2009).

²⁴H. Wang, T. X. Wu, X. Zhu, and S.-T. Wu, *J. Appl. Phys.* **95**, 5502 (2004).

²⁵S. T. Wu, *Appl. Phys. Lett.* **57**, 986 (1990).

²⁶M. Emoto, Y. Kusakabe, and M. Sugawara, *J. Display Technol.* **10**, 635 (2014).

²⁷Y. Chen, Z. Luo, F. Peng, and S.-T. Wu, *J. Display Technol.* **9**, 74 (2013).

²⁸Z. Luo, F. Peng, H. Chen, M. Hu, J. Li, Z. An, and S.-T. Wu, *Opt. Mater. Express* **5**, 603 (2015).

²⁹C. Murawski, K. Leo, and M. C. Gather, *Adv. Mater.* **25**, 6801 (2013).

³⁰C. Féry, B. Racine, D. Vaufrey, H. Doyeux, and S. Cina, *Appl. Phys. Lett.* **87**, 213502 (2005).

³¹G. Verzellesi, D. Saguatti, M. Meneghini, F. Bertazzi, M. Goano, G. Meneghesso, and E. Zanoni, *J. Appl. Phys.* **114**, 071101 (2013).

³²J.-I. Ohwada, *Inf. Disp.* **6**, 24 (2004).

³³J. I. Hirakata, A. Shingai, Y. Tanaka, K. Ono, and T. Furuhashi, *SID Symp. Dig. Tech. Pap.* **32**, 990 (2001).

³⁴T. Yamamoto, S. Sasaki, Y. Igarashi, and Y. Tanaka, *J. Soc. Inf. Disp.* **14**, 933 (2006).